



Meteorological influence on surface ozone trends in China: Assessing uncertainties caused by multi-dataset and multi-method

- 3 Xueqing Wang¹, Jia Zhu^{1*}, Guanjie Jiao¹, Xi Chen¹, Zhenjiang Yang¹, Lei Chen^{1,2}, Xipeng Jin¹, and Hong
- 4 Liao¹

10

28

- 5 ¹Jiangsu Key Laboratory of Atmospheric Environment Monitoring and Pollution Control, Jiangsu Collaborative Innovation
- 6 Centre of Atmospheric Environment and Equipment Technology, Joint International Research Laboratory of Climate and
- 7 Environment Change, School of Environmental Science and Engineering, Nanjing University of Information Science and
- 8 Technology, Nanjing, 210044, China
- 9 2State Environmental Protection Key Laboratory of Sources and Control of Air Pollution Complex, Beijing, China
- 11 Correspondence: Jia Zhu (jiazhu@nuist.edu.cn)
- 12 **Abstract.** China has witnessed notable increases in surface ozone (O₃) concentrations since 2013, with meteorology identified
- 13 as a critical driver. However, meteorological contributions vary with different meteorological datasets and analytical methods,
- and their uncertainties remain unassessed. This study leveraged decadal observational O₃ records (2013–2022) across China,
- 15 revealing intensified nationwide O₃ pollution with increasing O₃ trends of 0.79–1.31 ppb yr⁻¹ during four seasons. We gave
- special focus on uncertainties of meteorology-driven O₃ trends by using diverse meteorological datasets (ERA5, MERRA2,
- 17 FNL) and diverse analytical methods (Multiple Linear Regression, Random Forest, GEOS-Chem model). A useful statistic
- 18 (coefficient of variation, CV) was adopted as an uncertainty quantification metric. For multi-dataset analysis, models driven
- 19 by different meteorological datasets exhibited the maximum meteorology-driven O₃ trend (+0.55 ppb yr⁻¹, multi-dataset mean)
- with the highest consistency (CV=0.25) in spring. The FNL-driven model always obtained larger trends compared to ERA5
- 21 and MERRA2, which could be attributed to inability to accurately evaluate planetary boundary layer height in FNL dataset.
- 22 For multi-method analysis, three methods demonstrated optimal consistency in winter (CV=0.40) and the worst consistency
- 23 in summer (CV=2.00). The meteorology-driven O₃ trends obtained from GEOS-Chem model were almost smaller than those
- 24 obtained by other two methods, partly resulting from higher simulated O₃ values before 2018. Overall, all analyses driven by
- 25 diverse meteorological datasets and analytical methods drew a robust conclusion that meteorological conditions almost boosted
- 26 O₃ increases during all seasons; the uncertainties caused by different analytical methods were larger than those caused by
- 27 diverse meteorological datasets.

29 **Keywords:** Meteorological impact, O₃ trend, Uncertainty





1 Introduction

30

31

32

52

53

54

55

33 air pollutants exhibited decreases due to the emission control efforts, but not ozone (O₃) (Qi et al., 2023; Shen et al., 2020).In China, O₃ concentrations were increased by 50–124 μg m⁻³ from 2015 to 2022 (Yao et al., 2024). The formation of surface O₃ 34 depends nonlinearly on its precursors and is strongly influenced by meteorological conditions and anthropogenic emissions 35 36 (Wang et al., 2017). The impact of emission-related factors on O₃ increase in China over the past decade has been extensively 37 debated, including the ineffective control of volatile organic compounds (VOCs) emissions, the heightened O₃ photochemical 38 production due to the rapid decrease in PM_{2.5}, and the reduced nitric oxide (NO) titration effect (Li et al., 2019, 2022; Lin et 39 al., 2021a; Liu and Wang, 2020b; Ren et al., 2022). 40 Meteorological conditions also play a crucial role in shaping surface O₃ trends (Liu et al., 2023; Lu et al., 2019b), resulting in 41 increased O₃ concentrations during warm seasons over most of the United States, the European Union, and China from 2014 to 2019 (Lyu et al., 2023). In China, the meteorological impacts on O₃ levels may be comparable to the anthropogenic 42 43 contributions (Li et al., 2020; Liu and Wang, 2020a). From 2013 to 2018, meteorology could account for 43% of the daily 44 variability in summer surface O₃ concentrations in eastern China (Han et al., 2020). Adverse meteorological conditions were 45 identified as the cause of the worsening O₃ trends during 2015–2020 in Beijing-Tianjin-Hebei (BTH), Yangtze River Delta (YRD), and Pearl River Delta (PRD) regions (Hu et al., 2024b). In YRD, Dang et al. (2021) found that meteorological factors 46 47 contributed 84% of the O₃ increase during the summers of 2012–2017. In PRD, meteorological conditions contributed 83% of 48 the increasing O₃ trends during the summers of 2015–2019 (Mousavinezhad et al., 2021). After 2019, meteorological 49 conditions tended to improve O₃ air quality (Liu et al., 2023; Wang et al., 2023). Compared to 2019, the wetter and cooler 50 meteorological conditions in 2020 reduced O₃ concentrations by 2.9 ppb in eastern China (Yin et al., 2021). However, during 51 2022's summer, a notable rebound in O₃ levels occurred with O₃ concentrations rising by 12–15 ppb in China compared to

Since 2013, the Chinese government has implemented a series of policies to mitigate air pollution resulting from the repaid

industrial and urban expansion, such as the "Air Pollution Prevention and Control Action Plan" (Wang, 2021). Several criteria

Studies conducted over the past six years to determine the meteorological influence on the surface O₃ trend have been systematically reviewed, as documented in **Table S1**. The meteorological influence on surface O₃ concentrations is commonly assessed by using the traditional statistical model (TSM), machine learning model (MLM), and chemical transport model (CTM), driven by reanalysis meteorological products such as the fifth-generation European Centre for Medium-Range Weather Forecasts atmospheric reanalysis of the global climate (ERA5), the Modern-Era Retrospective Analysis for Research and Applications, version 2 (MERRA2), and the National Centres for Environmental Prediction (NCEP) Final Operational

2021, which was attributable to the extreme heatwave events (Qiao et al., 2024). With climate change, the frequency of extreme

O₃ pollution events is expected to increase (Gao et al., 2023; Ji et al., 2024). Given the shifted meteorological effects on O₃

and climate change, it is imperative to conduct O₃-Meteorology researches focusing on longer time frames to gain deeper

insights into the long-term changes in O₃ concentrations (Wang et al., 2024a).



66

82

85

88



62 Global Analysis data (FNL). Although several studies have demonstrated that meteorological impacts derived from CTM

63 results can corroborate the results of TSM (Liu et al., 2023; Yan et al., 2024) or MLM (Ni et al., 2024; Yin et al., 2021),

of uncertainties in the determination of meteorological effects on surface O₃ concentrations cannot be neglected. For example,

65 Pan et al. (2023) reported that the meteorological impact on O_3 trends in Beijing during 2013–2020 was +0.52 ppb yr⁻¹, which

is only half of the value estimated by Gong et al. (2022).

67 Uncertainties in quantifying the drivers of O₃ trends can be ascribed to the discrepancies between different meteorological

datasets and between different methods (Guo et al., 2021; Weng et al., 2022; Yao et al., 2024). Regarding the uncertainty

69 caused by different meteorological datasets, the meteorologically driven annual variations of O₃ concentrations from 2017 to

70 2019 identified by the MERRA2-driven TSM are not consistent with the ERA5-driven TSM during the summer of YRD (Hu

71 et al., 2024a; Qian et al., 2022). During the summer of 2013–2019 in YRD, Li et al. (2019) reported a trend of +0.7 ppb yr⁻¹

72 in meteorology-driven O₃ concentrations using the MERRA2-driven TSM, while the trend of Yan et al. (2024) was –0.3 μg

73 m⁻³ yr⁻¹ using the ERA5-driven TSM. Regarding the uncertainty caused by different methods, the meteorology-driven O₃ trend

74 identified by MLM for 2019–2021 was 2.4 times larger than that identified by CTM based on the same meteorological dataset

75 input (MERRA2) in the North China Plain (NCP) during summer (Wang et al., 2024a). In BTH, from 2021 to 2022, Luo et al.

76 (2024) identified a negative meteorological contribution based on the ERA5-driven MLM, while Yan et al. (2024) suggested

77 a positive contribution ($+4.3 \mu g m^{-3}$) based on the ERA5-driven TSM during summer.

78 On the basis of the above-mentioned, large uncertainties caused by multi-dataset or multi-method exist in O₃-Meteorology

79 analyses. However, available intercomparisons of O₃ analyses mainly focused on predicting the O₃ concentrations. For

80 example, Wang et al. (2024b) and Weng et al. (2023) compared the differences in O₃ concentration prediction caused by

81 different dataset and models, respectively. The uncertainties in quantifying the meteorological contributions to O₃ trends

caused by multi-dataset and multi-method remain unassessed. In addition, previous studies have predominantly focused on

83 summer O₃ pollution, although reports indicate an extension of the O₃ pollution season to winter and spring across major

84 clusters in China (Cao et al., 2024a; Li et al., 2021) and an unfavourable meteorological impact on O₃ air quality in spring and

winter in BTH (Luo et al., 2024). It is essential to conduct an intercomparison of meteorology-driven O₃ quantification using

86 multi-dataset and multi-method across all seasons.

87 This study utilized 10-year (2013–2022) surface O₃ observations in China to investigate long-term O₃ trends and quantify the

meteorological influence on O₃ trends using diverse meteorological datasets and analytical methods. Figure 1 shows the

89 framework and the main objectives were: (1) to assess uncertainties in identifying the meteorological influences caused by

90 multi-dataset. This was achieved by employing the TSM (i.e. multiple linear regression, MLR) driven by different reanalysis

91 meteorological products (i.e. ERA5, MERRA2, and FNL); (2) to assess uncertainties in identifying meteorological effects

92 caused by multi-method. This was achieved by establishing three models corresponding to TSM (i.e. MLR), MLM (i.e. random

93 forest, RF), and CTM (i.e. GEOS-Chem, GC), each driven by the MERRA2 product; (3) to calculate the mean of meteorology-





94 driven O₃ trends driven by three datasets (multi-dataset mean) and three methods (multi-method mean) to derive relatively robust results.

Our paper is structured as follows: Section 2 briefly introduces the details of surface O_3 observations and different meteorological datasets, as well as the framework of three methods, namely MLR, RF, and GC. The quantification of the uncertainties in the meteorology-driven O_3 trends caused by multi-dataset and multi-method is presented in Section 3. Section 4 concludes the paper. The findings of this study provide a scientific foundation for developing regional and seasonal strategies to mitigate and manage O_3 pollution in China.

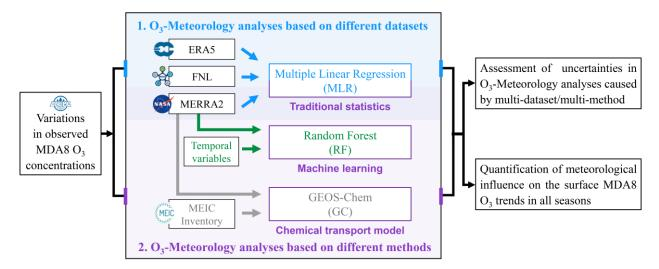


Figure 1. The framework of the uncertainty assessment in this study.

2 Data and Methods

2.1 Surface O₃ and meteorological data sources

Hourly surface O₃ observations from over 1000 state-controlled stations operated by the China National Environmental Monitoring Centre from 2013 to 2022 were used to analyze the long-term O₃ trends across all seasons: spring (March-April-May), summer (June-July-August), autumn (September-October-November), and winter (December-January-February). The maximum daily 8-hour average (MDA8) O₃ was calculated as an air quality indicator after filtering out abnormal data using the z-scores method. For detailed information on data quality control, refer to He et al. (2017).

In this study, we selected three widely used reanalysis products to assess the uncertainties caused by different meteorological datasets. Variables during 2013–2022 from ERA5, MERRA2, and FNL, as detailed in **Table S2**, were selected as meteorological inputs for building MLR models. These reanalyses have spatial resolutions of 0.25 °×0.25 °, 0.625 °×0.5 °, and





- 113 1 °×1 ° on a global latitude-longitude grid, respectively. In Section 3.2, we have also incorporated the NCEP FNL reanalysis
- product with a spatial resolution of 0.25 °×0.25 ° (FNL025) for the period 2016–2022 to explore the effect of spatial resolution
- on the analysis of uncertainties caused by multi-dataset.

116 2.2 Methods for obtaining long-term series and meteorological influence

117 2.2.1 Kolmogorov–Zurbenko (KZ) filter

- 118 The KZ filter, known for its ability to extract low frequency signals from time series data and handle missing values, has been
- 119 extensively applied in analyzing air quality variations (Eskridge et al., 1997; Rao and Zurbenko, 1994; Wise and Comrie,
- 120 2005). This filter is particularly useful in studying variations in air quality over time. The original time series of air pollutants
- 121 or meteorological variables (X(t)) can be decomposed by the KZ filter into the following form:

$$X(t) = X_{ST}(t) + X_{SN}(t) + X_{LT}(t)$$
(1)

$$X_{LT}(t) = KZ_{(365,3)}X(t) \tag{2}$$

$$X_{BL}(t) = KZ_{(15.5)}X(t) \tag{3}$$

$$X_{ST}(t) = X(t) - X_{BL}(t) \tag{4}$$

- In the decomposition process, X(t) represents the original time series, while $X_{ST}(t)$, $X_{SN}(t)$, and $X_{LT}(t)$ denote the short-
- term, seasonal, and long-term components, respectively. The baseline component, $X_{BL}(t)$, is defined as the sum of $X_{SN}(t)$ and
- 124 $X_{LT}(t)$. The $KZ_{(p,q)}$ filter executes q iterations with p as the moving average window length of the X(t) series. Specially, the
- 125 $X_{LT}(t)$ series is derived using the $KZ_{(365,3)}$ filter, capturing long-term changes with periods exceeding 1.7 years. The $X_{BL}(t)$
- series is obtained through the $KZ_{(15,5)}$ filter, while the $X_{ST}(t)$ series represents short-term fluctuations with period less than
- 127 33 days in the original time series. The KZ filter can fill in missing values by using iterated moving average technique.
- 128 Although not all of the ozone measurement sites were active over the entire period 2013–2022, missing value problem can be
- handled for most stations after we conduct three iterations with 365-day moving average.
- In this study, the $KZ_{(365,3)}$ filter was applied to extract the long-term trends in observed, meteorology-driven, and emission-
- driven MDA8 O₃ concentrations (see details in Fig. S1) during 2013–2022, as detailed in Sections 2.2.2, 2.2.3, and 2.2.4.

132 2.2.2 Stepwise MLR for separating meteorological influence

- As vividly illustrated in Fig. S1, a data-based TSM (i.e., MLR integrating the KZ filter) was employed to separate the observed
- 134 MDA8 O₃ concentrations into meteorology-driven and emission-driven concentrations (Sadeghi et al., 2022; Shang et al., 2023;
- 135 Zhang et al., 2022a). We initially applied the KZ filter to disassemble the MDA8 O₃ time series and all meteorological variables
- 136 listed in Table S2 into short-term, baseline, and long-term components at individual state-controlled stations for each season.
- 137 Subsequently, a series of screening processes aligned with our previous research (Wang et al., 2024c), were executed to





- 138 perform stepwise MLR on the short-term/baseline MDA8 O₃ concentrations and a group of meteorological variables series,
- 139 respectively. The established MLR model is presented herein:

$$C_{s,r}(t) = b_{0,s,r} + \sum_{i=1}^{k} b_{i,s,r} \times Met_i(t) + \varepsilon$$
(5)

- Here, $C_{s,r}(t)$ represents the MDA8 O₃ concentration for season s and monitoring station r, while $Met_i(t)$ signifies the i-th
- 141 meteorological variable out of a total of k, and $b_{i,s,r}$ is the corresponding regression coefficient. $b_{0,s,r}$ denotes the intercept
- 142 term, and ε is the residual term.
- 143 Finally, MLR models driven by meteorological variables from ERA5, MERRA2, or FNL will be constructed, allowing a
- 144 comprehensive analysis of multi-dataset uncertainties. The meteorological impact on O₃ trends derived from the MERRA2-
- driven MLR model will also be integrated into the analysis of multi-method uncertainties to improve the comparability of
- 146 results.

2.2.3 Random forest (RF) for deriving meteorological influence

- 148 The application of MLM in O₃ air quality research is becoming increasingly prevalent due to its superior accuracy, user-
- friendly nature, and capability to capture nonlinear relationships (Ni et al., 2024; Yao et al., 2024; Zhang et al., 2022b).
- 150 Considering the limited influence of discrepancy in O₃-Meteorology analyses stemming from different machine learning
- 151 algorithms (Wang et al., 2024a), we opted to build a representative MLM known as the meteorological normalisation model
- based on the RF algorithm (Ding et al., 2023; Ji et al., 2024; Zhang et al., 2023), to delineate meteorology- and emission-
- 153 driven O₃ concentrations.
- 154 RF stands out as a tree-based ensemble learning algorithm adept at handling nonlinear issues and reducing overfitting (Breiman,
- 155 2001). An RF model was developed for each state-controlled station in each season to predict the MDA8 O₃ concentration
- 156 using the Python package "Sklearn-RandomForestRegressor". The predictors included six temporal variables (year, month of
- 157 a year, day of a week, day of a month, day of a year, Unix time), serving as proxies for anthropogenic emission intensity
- 158 (Grange et al., 2018), alongside six MERRA2 meteorological variables as listed in Table S2 (i.e. SLP, T2max, U10, V10,
- 159 RH2, PBLHday). The training dataset comprised 70% of the data, while the remaining 30% was reserved for model evaluation.
- 160 A statistical cross-validation technique was employed to determine optimal hyperparameters for enhancing RF prediction
- performance (Weng et al., 2022). Coefficient of determination (R²) values were utilized to assess model performance for each
- station, with stations exhibiting $R^2 < 0.5$ (marked in blue in Fig. S2b) being excluded to ensure model credibility.
- After establishing the RF model, both the original time variables and resampled meteorological variables were utilized as input
- data. The meteorological variables were resampled by randomly selecting data from the two weeks before and after the
- specified date. To derive the de-weathered MDA8 O₃ concentration for a given day (e.g., March 1, 2013), the random
- 166 resampling process was iterated a thousand times. Our methodology closely follows that of Vu et al. (2019), with a more



169



- detailed process shown in Fig. S2(a). The meteorology-driven MDA8 O₃ concentrations were computed as the difference
- between the observed concentrations and de-weathered concentrations (i.e. emission-driven MDA8 O₃ concentrations).

2.2.4 GEOS-Chem (GC) simulation for quantifying meteorological influence

- 170 The numerical analysis of surface O_3 in China was performed with the GC classic version 13.3.3
- 171 (https://github.com/geoschem/GCClassic/releases/tag/13.3.3). Developed as a global 3-D model, GC incorporates a fully
- 172 coupled O₃-NOx-VOCs-aerosol-halogen chemical mechanism, driven by the MERRA2 meteorological input. Numerous
- 173 studies have leveraged GC to simulate O₃ air quality in China, demonstrating alignment between observational data and model
- outcomes (Dai et al., 2024; Dang et al., 2021; Li et al., 2019; Lu et al., 2019a). We employed the nested-grid GC to simulate
- 175 the long-term surface O₃ concentrations and to quantify the meteorology-driven MDA8 O₃ trends over China. The nested-grid
- domain was set over China's mainland (15–55 %, 70–140 Ξ) with a horizontal resolution of 0.5 °latitude by 0.625 °longitude
- and 47 vertical layers extending up to an altitude of 0.01 hPa. A global simulation with a horizontal resolution of $2^{\circ}\times2.5^{\circ}$
- 178 provided the chemical boundary conditions for the nested-grid simulation every 3 hours. To ensure model stability and
- accuracy, a 6-month spin-up simulation was conducted before the commencement of the targeted 10-year period from March
- 180 2013 to February 2023.
- 181 Emissions management within GC is facilitated by the Harmonized Emissions Component, a system introduced by (Lin et al.,
- 182 2021b). Anthropogenic emissions are sourced from the Community Emissions Data System (CEDS) inventory globally, with
- 183 specific overwriting by the Multi-resolution Emission Inventory for China (MEIC) within the Chinese region. The simulations
- 184 for 2021–2022 adopt a similar approach to Zhai et al. (2021), using 2019 MEIC emissions with NOx emissions reduced by 8
- 185 ~ 13% and 2017 MEIC with VOCs emissions reduced by 10 ~ 14%, based on the policy released by Ministry of Ecology and
- 186 Environment of the People's Republic of China. For natural emissions, biogenic VOCs, soil, and lightning NOx were calculated
- 187 online in the model. Emissions from biomass burning, ships, and aircraft are sourced from the Global Fire Emissions Database,
- 188 the CEDS inventory, and the 2019 Aircraft Emissions Inventory Code, respectively.
- 189 In order to assess the model's performance and to get a quantification of meteorology-driven O₃ trends during the period of
- 190 2013–2022, two sets of simulations were conducted: (1) BASE: the standard simulation of O₃ concentrations from 2013 to
- 191 2022, where both meteorological fields and emissions (including anthropogenic, natural, and biomass emissions) vary year by
- 192 year from 2013 to 2022; (2) FixE2013: a "fixed-emission simulation" where meteorological conditions vary from 2013 to
- 193 2022 while anthropogenic emissions remain constant at 2013 levels. The FixE2013 simulation is designed to quantify the
- meteorological influence on O₃ variations. Figure S3 evaluates the performance of the GC simulation for 2013–2022. The GC
- 195 model generally captures the monthly variability in MDA8 O₃ over China and three cluster megacities, with the correlation
- 196 coefficients greater than 0.80, although it always shows a high bias of surface O₃ in warm seasons (Dai et al., 2024), which



199

200

201

202

203

204205

206207

208

209

210



can be attributed to its inability to capture the complex terrain, local pollution sources and meteorological conditions, or overestimates of the correlations between the surface O₃ concentration and temperature (Shen et al., 2022; Sun et al., 2021).

2.3 Assessment of uncertainties caused by multi-dataset and multi-method

In this study, the coefficient of variation (CV) is applied to assess the uncertainties in O₃-Meteorology analyses caused by different meteorological datasets or methods. The CV, calculated as the ratio of the standard deviation to the mean, serves as a statistical metric commonly utilized to measure the diversity within datasets or models (Bedeian and Mossholder, 2000; Chen et al., 2019). In this study, higher CVs indicate lower consistency of meteorologically driven O₃ trends derived from different datasets or methods. Given the possibility of disparate meteorology-driven O₃ trends detected by different datasets or methods, we consider the absolute value of the CV as a quantitative indicator of the uncertainties. When examining the uncertainties arising from different datasets, the CV represents the standard deviation of trends derived from the ERA5, MERRA2, and FNL-driven MLR models divided by the mean. Similarly, in the context of multi-method uncertainties, the CV is the standard deviation of trends identified by the MLR, RF, and GC models divided by the mean.

3 Results

3.1 Observed trends in surface O₃ concentration

- 211 Figure 2 shows the trends in observed MDA8 O₃ concentrations over a 10-year period during four seasons. Noteworthy
- 212 increases in O₃ concentrations were observed at 78 ~ 93% of state-controlled stations over the years, with the national trend
- being +1.31 ppb yr⁻¹, +0.93 ppb yr⁻¹, +0.79 ppb yr⁻¹, and +0.80 ppb yr⁻¹ in spring, summer, autumn, and winter, respectively.
- 214 The major eastern megacity clusters in China also displayed their highest MDA8 O₃ increase trends in spring, with trends of
- 215 +1.16 ppb yr⁻¹ in BTH, +1.61 ppb yr⁻¹ in YRD, and +1.48 ppb yr⁻¹ in PRD, which has been reported in previous studies (Cao
- 216 et al., 2024b; Chen et al., 2020; Wang et al., 2022). During summer, BTH and YRD faced more severe challenges in O₃
- 217 prevention and control compared to PRD, with rising MDA8 O₃ trends in the former two regions being about three times
- 218 higher than that in PRD (Fig. 2b).
- 219 In terms of O₃ growth rates, Shanxi province and Anhui province ranked the top two provinces in China over the past decade
- 220 in all seasons except for winter, consistent with Zhao et al. (2020). In spring and winter, O₃ concentrations increased in all
- 221 provinces, with trends of $+0.39 \sim +2.75$ ppb yr⁻¹ and $+0.42 \sim +1.30$ ppb yr⁻¹, respectively. Notably, Jilin province experienced
- 222 an obvious improvement in O_3 air quality during summer and autumn, with decreasing trends of -0.74 ppb yr⁻¹ and -0.38 ppb
- 223 yr⁻¹, respectively, which was also confirmed by Gong et al. (2022).





The annual and seasonal mean MDA8 O_3 concentrations across China are detailed in **Fig. S4** and **Fig. S5**, providing a holistic depiction of the persisting spread of O_3 pollution since 2013. On a national average, the O_3 air quality was worst in summer, with the average O_3 levels exceeding the air quality standard Grade I limit of 50 ppb almost every year. Notably, the summer of 2019 marked a peak period for O_3 pollution, with an average concentration of 59.7 ppb (**Fig. S5b**).

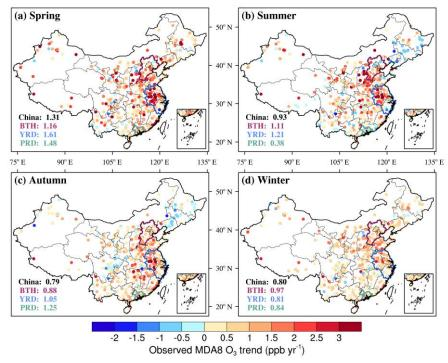


Figure 2. Trends in observed MDA8 O_3 concentrations in China from 2013 to 2022 during (a) spring, (b) summer, (c) autumn, and (d) winter. Values in black, purple, blue, and green represent the mean trends for the whole China, BTH, YRD, and PRD, respectively.

3.2 Uncertainty in meteorology-driven O₃ trends caused by multi-dataset

The traditional statistical method (the MLR model), which has a relatively low computational cost but can provide valuable insights into the quantification of meteorological contributions to O₃ trends, was used to investigate the uncertainties in O₃-Meteorology analyses caused by different meteorological datasets. As shown in **Fig. 3(a)**, meteorological conditions contribute to an increase in MDA8 O₃ concentrations across all seasons in China, with the multi-dataset mean trends ranging from +0.19 ppb yr⁻¹ to +0.55 ppb yr⁻¹. All three dataset-driven MLR models indicate that meteorology leads to the most rapid increase in MDA8 O₃ concentrations in spring, with trends ranging from +0.47 ppb yr⁻¹ to +0.71 ppb yr⁻¹, and a low CV of 0.25. This suggests a high consistency among the three datasets in assessing the meteorological influence on surface O₃ concentrations. During summer and autumn, relatively higher CVs were shown, indicating larger variability, despite lower meteorological influences on O₃ trends. Specifically in autumn, the meteorology-driven O₃ trend derived from the FNL-driven MLR model is 4.1 times larger than that derived from the ERA5-driven MLR model.





Figure 3(b-d) depicts the meteorological impact on the MDA8 O₃ trends in the three megacity clusters (BTH, YRD, and PRD). Meteorology caused the MDA8 O₃ increase in most of the megacity clusters and seasons, except for BTH during autumn. In seasons where the meteorological effects derived from the three MLR models are all positive, the multi-dataset mean trends ranged from +0.09 to +0.33 ppb yr⁻¹ in BTH, +0.18 to +0.68 ppb yr⁻¹ in YRD, and +0.73 to +1.13 ppb yr⁻¹ in PRD. Consistent with Fig. 3(a), meteorology triggered the most rapid increase in MDA8 O₃ concentrations in spring across the three megacity clusters. The largest meteorological impact in BTH during spring was also revealed by Luo et al. (2024). Large CVs (>1.0) were observed in BTH during summer and autumn. Notably, the meteorological influence calculated by the three dataset-driven MLR models even showed opposite trends in BTH during autumn, indicating challenges in assessing the meteorological impacts on surface O₃ concentrations. In contrast, in YRD and PRD, the three MLR models demonstrated high consistency across almost all seasons. Although the largest CV reached 4.4 in PRD during summer, it was considered acceptable because the three MLR models indicated that meteorology had a minor influence (less than +0.1 ppb yr⁻¹) on O₃ trends.

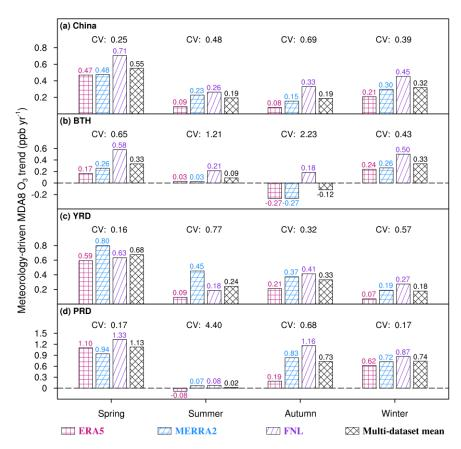


Figure 3. Meteorology-driven MDA8 O₃ trends in (a) the whole China, (b) BTH, (c) YRD, and (d) PRD during four seasons. Values in red, blue, and purple represent trends calculated by ERA5-, MERRA2-, and FNL-driven multiple linear regression (MLR) model, respectively. The fourth black bar represents the multi-dataset mean trend. The absolute value of coefficient of variation (CV) for each season is also shown.





From a provincial perspective in **Fig. S6**, we can also see that the meteorological contributions to O_3 trends are positive during spring and winter. Large uncertainties in O_3 -Meteorology analyses were identified during summer and autumn. There were 7 and 12 provinces with controversial meteorological contributions identified by the three dataset-driven MLR models in summer and autumn, respectively.

Figure 4 displays the spatial distribution of the CV values from the perspective of state-controlled stations in four seasons. Consistent with the national and provincial perspectives, the least uncertainties in O_3 -Meteorology analyses were observed in spring, with CVs less than 0.5 at 45% of stations. Obvious discrepancies in meteorology-driven O_3 trends are found in summer and autumn, particularly in the NCP and northwestern China, with CVs greater than 1.0 at 33 ~ 40% of the stations. In autumn, it is noteworthy that the uncertainties caused by multi-dataset are lower in the south than in the north. In a study using the MLR model to predict O_3 concentration, it was also found that the MLR had better performance in the south than in the north (Han et al., 2020).

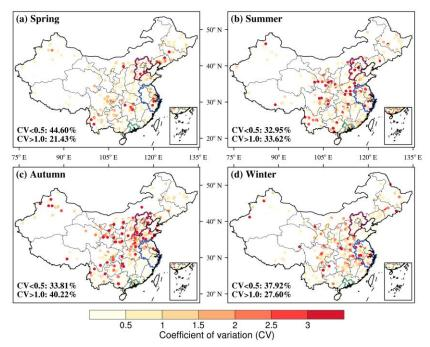


Figure 4. The absolute value of coefficient of variation (CV) for each state-controlled monitoring station in China during (a) spring, (b) summer, (c) autumn, and (d) winter. The CV is calculated by the standard deviation of the trends derived from ERA5-, MERRA2-, and FNL-driven MLR models divided by the mean. The darker colour means the larger uncertainty in quantifying the meteorological impact on observed O₃ trends. The proportion of state-control stations with CV less than 0.5 and greater than 1.0 is also shown. The outline marked in purple, blue, and green represents the region of BTH, YRD, and PRD, respectively.

Based on the three dataset-driven MLR models, the meteorological and anthropogenic contributions to the MDA8 O₃ trends in China during 2013–2022 were further examined. As presented in **Fig. 5**, both meteorological conditions and anthropogenic





emissions lead to O₃ increases. According to the ERA5- and MERRA2-driven MLR models, variations in anthropogenic emissions were identified as the dominant factor driving the increase in MDA8 O₃ concentrations across all seasons, with anthropogenic contributions ranging from 63.2% to 90.4%. The results suggest that more stringent emission control policies should be implemented to counteract the adverse effects of meteorological influences on O₃ concentrations.

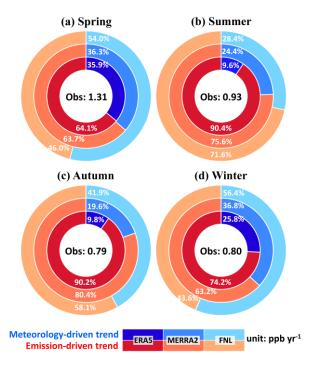


Figure 5. Percentage contributions of meteorological conditions (blue) and anthropogenic emissions (red) to the trends in observed MDA8 O₃ concentrations calculated by ERA5-, MERRA2-, and FNL-driven multiple linear regression (MLR) model in China during (a) spring, (b) summer, (c) autumn, and (d) winter. Values in black represent the observed MDA8 O₃ trends averaged over the whole China.

It is interesting to note that the FNL-driven model almost always gave relatively larger predictions of meteorologically driven O₃ trends compared to the models driven by ERA5 and MERRA2. To investigate whether this discrepancy was due to the coarser spatial resolution of the FNL dataset, a comparison was made between the FNL025-driven MLR model (0.25 °×0.25 °) and the FNL-driven MLR model (1.0 °×1.0 °). As depicted in **Fig. S7**, the deviation of the meteorology-driven trends calculated by the two MLR models was less than 0.1 in China and three megacity clusters across four seasons, indicating that different spatial resolutions have little effect on O₃-Meteorology analyses. Further examination was conducted to assess the influence of meteorological variables on O₃-Meteorology analyses. **Table S3** lists the 10-year trends in each meteorological factor and shows a great discrepancy in the variable "PBLHday". Zuo et al. (2023) also reported that FNL exhibited the highest uncertainty for the evaluation of PBLH compared to ERA5 and MERRA2. As **Fig. S8** shows, constructing the FNL-driven MLR models using six meteorological variables without "PBLHday" can reduce the estimated meteorological impact by 0.08





to 0.20 ppb yr⁻¹. To obtain a more reliable estimate, it is recommended to avoid using "PBLH" to build the FNL-driven MLR models when separating meteorological and anthropogenic influences on O₃ concentrations in China.

3.3 Uncertainty in meteorology-driven O₃ trends caused by multi-method

This section discusses the uncertainties caused by multi-method (i.e. MLR, RF, GC), all of which are driven by the MERRA2 dataset. **Figure 6** illustrates the meteorology-driven MDA8 O_3 trends calculated by the MLR, RF, and GC models. For the whole China, the large uncertainties were evident during summer, when the meteorology-driven O_3 trends derived from the MLR model are notably larger than those from the RF and GC models, with a CV of 2.0 (**Fig. 6a**). In the other three seasons, although the multi-method mean trends, ranging from +0.17 to +0.26 ppb yr⁻¹, are 1.1 to 2.1 times lower than those computed by the three dataset-driven MLR models (**Fig. 3a**), all models converge on the conclusion that meteorological conditions contribute to the deterioration of O_3 air quality.

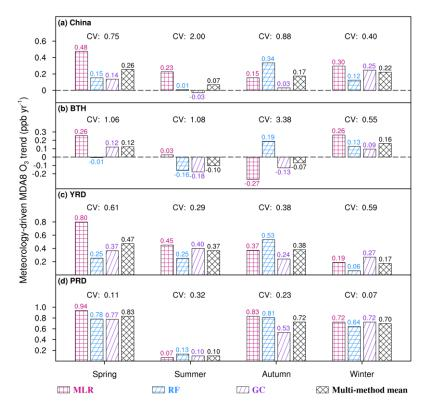


Figure 6. Meteorology-driven MDA8 O₃ trends in (a) the whole China, (b) BTH, (c) YRD, and (d) PRD during four seasons. Values in red, blue, and purple represent trends calculated by multiple linear regression (MLR), random forest (RF), and GEOS-Chem (GC) models, respectively. The fourth black bar represents the multi-method mean trend. The absolute value of coefficient of variation (CV) for each season is also shown.

In YRD and PRD, the three models exhibit strong agreement in all seasons, with the largest CV of 0.61, where meteorology leads to an increase in O_3 concentrations with multi-method mean trends of +0.17 to +0.47 ppb yr⁻¹ and +0.10 to +0.83 ppb yr⁻¹, respectively. Notably, the most rapid meteorology-driven O_3 increase is also observed in spring (**Fig. 6c and Fig. 6d**), which is consistent with **Fig. 3c and Fig. 3d**. In BTH, the three models perform consistently well only in winter, with meteorology-driven O_3 trends ranging from +0.09 to +0.26 ppb yr⁻¹ and a CV of 0.55. It is also observed that in summer and autumn, meteorology plays a relatively small role in influencing O_3 air quality despite the controversial results obtained by the three models (**Fig. 6b**). This finding aligns with a study focusing on the O_3 air quality in BTH from 2015 to 2022 (Luo et al., 2024), which suggested that meteorological conditions tend to increase MDA8 O_3 concentration by only 0.01 μ g m⁻³ in summer and decrease MDA8 O_3 concentration by 0.3 μ g m⁻³ in autumn from 2015 to 2022.

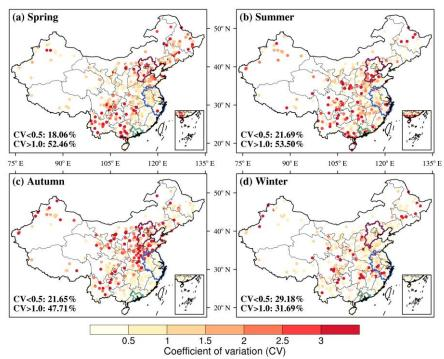


Figure 7. The absolute value of coefficient of variation (CV) for each state-controlled monitoring station in China during (a) spring, (b) summer, (c) autumn, and (d) winter. The CV is calculated by the standard deviation of the trends derived from multiple linear regression (MLR), random forest (RF), and GEOS-Chem (GC) models divided by the mean. The darker colour means the larger uncertainty in quantifying the meteorological impact on observed O₃ trends. The proportion of state-control stations with CV less than 0.5 and greater than 1.0 is also presented. The outline marked in purple, blue, and green represents the region of BTH, YRD, and PRD, respectively.

In addition, Fig. 6 illustrates that the meteorology-driven O₃ trends obtained from GC are relatively smaller. As shown in Fig. S3, this difference could partly be attributed to the higher O₃ values simulated by the GC model before 2018. It is crucial to take into account the overestimation of low-level O₃ observations, as noted in previous studies (Hu et al., 2024c; Mao et al.,



356



328 2024). To validate this hypothesis, we compared the meteorology-driven O₃ trends calculated by MLR with those calculated by GC from 2018 to 2022, and a higher agreement was found over 2018–2022 compared to the 2013–2022 period in Fig. S9. 329 From a provincial perspective, as depicted in Fig. S10, the three models together indicate that meteorology causes an O₃ 330 increase in winter across almost all provinces except for Guizhou and Sichuan. In summer and autumn, meteorology leads to 331 332 a decrease in 5 provinces, mainly in northeastern China, with trends ranging from -0.42 to -0.11 ppb yr⁻¹. Interestingly, across all seasons, the three models introduce less uncertainty in the developed east coast regions such as Jiangsu, Fujian, and 333 334 Guangdong compared to other provinces. This suggests that the impact of meteorology on O_3 levels in these developed regions along the east coast of China is relatively reliable. 335 336 From the perspective of state-controlled stations, Fig. 7 shows the spatial distribution of the CV during four seasons. The 337 lowest disparities in the meteorology-driven MDA8 O₃ trends persist in winter, with CVs of less than 0.5 recorded at 29% of the stations. In the other three seasons, however, significant discrepancies in meteorology-driven O₃ trends are prominent, with 338 339 a CV greater than 1.0 at least 48% of the stations. Similar to Fig. 4, it is noteworthy that in autumn, the uncertainties caused 340 by multi-method are more pronounced in the northern regions compared to the southern regions. **4 Conclusions and Discussions** 341 342 This study used the 10-year (2013–2022) surface O₃ observations to clarify O₃ variations during four seasons in China, and quantify the meteorological impacts on O₃ trends, with a special focus on the uncertainties of meteorology-driven O₃ trends. 343 344 Diverse meteorological datasets (ERA5, MERRA2, FNL) and analytical methods (MLR, RF, GEOS-Chem) were employed 345 to systematically analyze the uncertainties in meteorology-driven O₃ trends caused by multi-dataset and multi-method which 346 have not been assessed before. The coefficient of variation (CV) was adopted as a metric to assess the uncertainty. The main 347 conclusions are as follows: Over the past decade, increasing trends in MDA8 O₃ were observed at over 78% of state-controlled stations across all seasons, 348 with the national trend of +1.31 ppb yr⁻¹, +0.93 ppb yr⁻¹, +0.79 ppb yr⁻¹, and +0.80 ppb yr⁻¹ in spring, summer, autumn, and 349 350 winter, respectively. 351 We first applied the MLR model (driven by ERA5, MERRA2, and FNL, respectively), which has proven its usefulness and reliability in O₃-Meteorology analyses, to assess uncertainties caused by multi-dataset. For the whole China, all three dataset-352 driven MLR models indicate that meteorological conditions have led to an increase in MDA8 O₃ concentrations in four seasons, 353 with multi-dataset mean trends ranging from +0.19 ppb yr⁻¹ to +0.55 ppb yr⁻¹. The models driven by different meteorological 354 datasets showed a maximum meteorology-driven O₃ trend of +0.55 ppb yr⁻¹ with the highest consistency (CV=0.25) in spring. 355

The FNL-driven model always obtained larger meteorology-driven O₃ trends compared to the models driven by ERA5 and



370

371



- MERRA2, which could be attributed to the inability to accurately evaluate PBLH in the FNL dataset. The dominant influence 357 of anthropogenic emissions on O₃ increase was also identified, highlighting the need for more stringent emission control 358 359 policies to mitigate the adverse effects of meteorological conditions. We further applied the MLR, RF and GEOS-Chem model to obtain the meteorological influence on O₃ trends to explore the 360 uncertainties caused by multi-method. In China and three megacity clusters, the three methods consistently indicated positive 361 meteorological contributions to O₃ increases during spring and winter, with multi-method mean trends ranging from +0.12 to 362 363 +0.83 ppb yr⁻¹ and +0.17 to +0.70 ppb yr⁻¹, respectively. In summer and autumn, especially in BTH, where the meteorological influence was relatively lower, three methods gave conflicting predictions of meteorological influence on O₃ with CVs greater 364 than 1.08. For the whole China, three different methods demonstrated optimal consistency in winter with CV of 0.40 and the 365 366 worst consistency in summer with CV of 2.00. The meteorology-driven O₃ trends obtained from GEOS-Chem model were almost relatively smaller than those obtained by other two methods, which could partly be attributed to the higher O₃ values 367 368 simulated by the GEOS-Chem model before 2018. 369 All analyses driven by diverse meteorological datasets and analytical methods drew a consistent finding: meteorological
- While this study advances understanding of meteorological contributions to O₃ trends, there exist several limitations that should be overcome in future studies. More meteorological datasets and methods should be used to provide a more accurate assessment of uncertainties in O₃-Meteorology analyses. Considering that the favourable effects of meteorology on O₃ pollution tend to be weaker after 2019 and the effects of COVID-19, it is necessary to conduct research over different periods and longer periods. In addition, further research is needed to focus on the meteorological contributions to O₃ trends in northern China due to larger uncertainties.

different analytical methods were larger than those caused by diverse meteorological datasets.

conditions almost contribute to O₃ increase across all seasons. The uncertainties of meteorology-driven O₃ trends caused by

- 378 Data availability. The surface O₃ observations are obtained from https://quotsoft.net/air/. The ERA5, MERRA2, FNL, and 379 FNL025 reanalysis meteorological taken https://cds.climate.copernicus.eu/datasets, data are from 380 http://geoschemdata.wustl.edu/ExtData/GEOS_0.5x0.625_AS/MERRA-2/, https://rda.ucar.edu/datasets/d083002/, https://rda.ucar.edu/datasets/ds083-3/, respectively. The code of the GEOS-Chem (version 13.3.3) model is available at 381 382 https://zenodo.org/records/5748260.
- Author contributions. JZ designed the research, and XW performed simulations and analyzed the results. GJ, XC, and ZY helped with the model simulations. LC, XJ, and HL provided useful comments on the paper. XW and JZ wrote the paper with contributions from all co-authors.
- 386 **Competing interests.** The authors declare that they have no conflict of interest.





- 387 Financial support. This research has been supported by National Nature Science Foundation of China (No.42293323,
- 388 42007195, 42305121), National Key Research and Development Program of China (No.2022YFE0136100), State
- 389 Environmental Protection Key Laboratory of Sources and Control of Air Pollution Complex (No.SCAPC202114), and Natural
- 390 Science Foundation of Jiangsu Province (No.BK20220031).

391 References

- 392 Bedeian, A. G. and Mossholder, K. W.: On the use of the coefficient of variation as a measure of diversity, Organ. Res.
- 393 Methods, 3, 285–297, https://doi.org/10.1177/109442810033005, 2000.
- 394 Breiman, L.: Random forests, Mach. Learn., 45, 5–32, https://doi.org/10.1023/A:1010933404324, 2001.
- 395 Cao, T., Wang, H., Li, L., Lu, X., Liu, Y., and Fan, S.: Fast spreading of surface ozone in both temporal and spatial scale in
- 396 Pearl River Delta, J. Environ. Sci., 137, 540–552, https://doi.org/10.1016/j.jes.2023.02.025, 2024a.
- 397 Cao, T., Wang, H., Chen, X., Li, L., Lu, X., Lu, K., and Fan, S.: Rapid increase in spring ozone in the Pearl River Delta, China
- 398 during 2013-2022, npj Clim. Atmos. Sci., 7, 309, https://doi.org/10.1038/s41612-024-00847-3, 2024b.
- 399 Chen, L., Gao, Y., Zhang, M., Fu, J. S., Zhu, J., Liao, H., Li, J., Huang, K., Ge, B., Wang, X., Lam, Y. F., Lin, C.-Y., Itahashi,
- S., Nagashima, T., Kajino, M., Yamaji, K., Wang, Z., and Kurokawa, J.: MICS-Asia III: multi-model comparison and
- 401 evaluation of aerosol over East Asia, Atmos. Chem. Phys., 19, 11911–11937, https://doi.org/10.5194/acp-19-11911-2019,
- 402 2019.
- 403 Chen, L., Zhu, J., Liao, H., Yang, Y., and Yue, X.: Meteorological influences on PM_{2.5} and O₃ trends and associated health
- burden since China's clean air actions, Sci. Total Environ., 744, 140837, https://doi.org/10.1016/j.scitotenv.2020.140837,
- 405 2020.
- 406 Dai, H., Liao, H., Wang, Y., and Qian, J.: Co-occurrence of ozone and PM_{2.5} pollution in urban/non-urban areas in eastern
- 407 China from 2013 to 2020: roles of meteorology and anthropogenic emissions, Sci. Total Environ., 924, 171687,
- 408 https://doi.org/10.1016/j.scitotenv.2024.171687, 2024.
- 409 Dai, Q., Dai, T., Hou, L., Li, L., Bi, X., Zhang, Y., and Feng, Y.: Quantifying the impacts of emissions and meteorology on
- 410 the interannual variations of air pollutants in major Chinese cities from 2015 to 2021, Sci. China Earth Sci.,
- 411 https://doi.org/10.1007/s11430-022-1128-1, 2023.
- 412 Dang, R., Liao, H., and Fu, Y.: Quantifying the anthropogenic and meteorological influences on summertime surface ozone in
- 413 China over 2012–2017, Sci. Total Environ., 754, 142394, https://doi.org/10.1016/j.scitotenv.2020.142394, 2021.
- 414 Ding, J., Dai, Q., Fan, W., Lu, M., Zhang, Y., Han, S., and Feng, Y.: Impacts of meteorology and precursor emission change
- on O₃ variation in Tianjin, China from 2015 to 2021, J. Environ. Sci., 126, 506-516,
- 416 https://doi.org/10.1016/j.jes.2022.03.010, 2023.





- 417 Eskridge, R. E., Ku, J. Y., Rao, S. T., Porter, P. S., and Zurbenko, I. G.: Separating different scales of motion in time series of
- 418 meteorological variables, Bull. Am. Meteorol. Soc., 78, 1473–1483, https://doi.org/10.1175/1520-
- 419 0477(1997)078<1473:SDSOMI>2.0.CO;2, 1997.
- 420 Gao, M., Wang, F., Ding, Y., Wu, Z., Xu, Y., Lu, X., Wang, Z., Carmichael, G. R., and McElroy, M. B.: Large-scale climate
- patterns offer preseasonal hints on the co-occurrence of heat wave and O₃ pollution in China, Proc. Natl. Acad. Sci., 120,
- 422 e2218274120, https://doi.org/10.1073/pnas.2218274120, 2023.
- 423 Gong, S., Zhang, L., Liu, C., Lu, S., Pan, W., and Zhang, Y.: Multi-scale analysis of the impacts of meteorology and emissions
- on PM_{2.5} and O₃ trends at various regions in China from 2013 to 2020 2. Key weather elements and emissions, Sci. Total
- 425 Environ., 824, 153847, https://doi.org/10.1016/j.scitotenv.2022.153847, 2022.
- 426 Grange, S. K., Carslaw, D. C., Lewis, A. C., Boleti, E., and Hueglin, C.: Random forest meteorological normalisation models
- for Swiss PM₁₀ trend analysis, Atmos. Chem. Phys., 18, 6223–6239, https://doi.org/10.5194/acp-18-6223-2018, 2018.
- 428 Guo, J., Zhang, J., Yang, K., Liao, H., Zhang, S., Huang, K., Lv, Y., Shao, J., Yu, T., Tong, B., Li, J., Su, T., Yim, S. H. L.,
- Stoffelen, A., Zhai, P., and Xu, X.: Investigation of near-global daytime boundary layer height using high-resolution
- 430 radiosondes: first results and comparison with ERA5, MERRA-2, JRA-55, and NCEP-2 reanalyses, Atmos. Chem. Phys.,
- 431 21, 17079–17097, https://doi.org/10.5194/acp-21-17079-2021, 2021.
- 432 Han, H., Liu, J., Shu, L., Wang, T., and Yuan, H.: Local and synoptic meteorological influences on daily variability in
- summertime surface ozone in eastern China, Atmos. Chem. Phys., 20, 203–222, https://doi.org/10.5194/acp-20-203-2020,
- 434 2020.
- 435 He, X., Leng, C., Pang, S., and Zhang, Y.: Kinetics study of heterogeneous reactions of ozone with unsaturated fatty acid
- single droplets using micro-FTIR spectroscopy, RSC Adv., 7, 3204–3213, https://doi.org/10.1039/C6RA25255A, 2017.
- 437 Hu, F., Xie, P., Xu, J., Lv, Y., Zhang, Z., Zheng, J., and Tian, X.: Long-term trends of ozone in the Yangtze River Delta, China:
- 438 spatiotemporal impacts of meteorological factors, local, and non-local emissions, J. Environ. Sci., S1001074224003826,
- 439 https://doi.org/10.1016/j.jes.2024.07.017, 2024a.
- 440 Hu, T., Lin, Y., Liu, R., Xu, Y., Ouyang, S., Wang, B., Zhang, Y., and Liu, S. C.: What caused large ozone variabilities in
- three megacity clusters in eastern China during 2015-2020?, Atmos. Chem. Phys., 24, 1607-1626,
- 442 https://doi.org/10.5194/acp-24-1607-2024, 2024b.
- 443 Hu, W., Zhao, Y., Lu, N., Wang, X., Zheng, B., Henze, D. K., Zhang, L., Fu, T.-M., and Zhai, S.: Changing Responses of
- PM_{2.5} and Ozone to Source Emissions in the Yangtze River Delta Using the Adjoint Model, Environ. Sci. Technol., 58,
- 445 628–638, https://doi.org/10.1021/acs.est.3c05049, 2024c.
- 446 Ji, X., Chen, G., Chen, J., Xu, L., Lin, Z., Zhang, K., Fan, X., Li, M., Zhang, F., Wang, H., Huang, Z., and Hong, Y.:
- 447 Meteorological impacts on the unexpected ozone pollution in coastal cities of China during the unprecedented hot summer
- 448 of 2022, Sci. Total Environ., 914, 170035, https://doi.org/10.1016/j.scitotenv.2024.170035, 2024.
- 449 Li, K., Jacob, D. J., Liao, H., Shen, L., Zhang, Q., and Bates, K. H.: Anthropogenic drivers of 2013–2017 trends in summer
- 450 surface ozone in China, Proc. Natl. Acad. Sci., 116, 422–427, https://doi.org/10.1073/pnas.1812168116, 2019.





- Li, K., Jacob, D. J., Shen, L., Lu, X., De Smedt, I., and Liao, H.: Increases in surface ozone pollution in China from 2013 to
- 452 2019: anthropogenic and meteorological influences, Atmos. Chem. Phys., 20, 11423–11433, https://doi.org/10.5194/acp-
- 453 20-11423-2020, 2020.
- 454 Li, K., Jacob, D. J., Liao, H., Qiu, Y., Shen, L., Zhai, S., Bates, K. H., Sulprizio, M. P., Song, S., Lu, X., Zhang, Q., Zheng,
- B., Zhang, Y., Zhang, J., Lee, H. C., and Kuk, S. K.: Ozone pollution in the north China plain spreading into the late-
- winter haze season, Proc. Natl. Acad. Sci., 118, e2015797118, https://doi.org/10.1073/pnas.2015797118, 2021.
- 457 Li, X., Yuan, B., Parrish, D. D., Chen, D., Song, Y., Yang, S., Liu, Z., and Shao, M.: Long-term trend of ozone in southern
- 458 China reveals future mitigation strategy for air pollution, Atmos. Environ., 269, 118869,
- 459 https://doi.org/10.1016/j.atmosenv.2021.118869, 2022.
- 460 Lin, C., Lau, A. K. H., Fung, J. C. H., Song, Y., Li, Y., Tao, M., Lu, X., Ma, J., and Lao, X. Q.: Removing the effects of
- 461 meteorological factors on changes in nitrogen dioxide and ozone concentrations in China from 2013 to 2020, Sci. Total
- 462 Environ., 793, 148575, https://doi.org/10.1016/j.scitotenv.2021.148575, 2021a.
- 463 Lin, H., Jacob, D. J., Lundgren, E. W., Sulprizio, M. P., Keller, C. A., Fritz, T. M., Eastham, S. D., Emmons, L. K., Campbell,
- P. C., Baker, B., Saylor, R. D., and Montuoro, R.: Harmonized Emissions Component (HEMCO) 3.0 as a versatile
- emissions component for atmospheric models: application in the GEOS-Chem, NASA GEOS, WRF-GC, CESM2, NOAA
- 466 GEFS-Aerosol, and NOAA UFS models, Geosci. Model Dev., 14, 5487–5506, https://doi.org/10.5194/gmd-14-5487-
- 467 2021, 2021b.
- 468 Liu, Y. and Wang, T.: Worsening urban ozone pollution in China from 2013 to 2017 part 1: the complex and varying roles
- 469 of meteorology, Atmos. Chem. Phys., 20, 6305–6321, https://doi.org/10.5194/acp-20-6305-2020, 2020a.
- 470 Liu, Y. and Wang, T.: Worsening urban ozone pollution in China from 2013 to 2017 part 2: the effects of emission changes
- and implications for multi-pollutant control, Atmos. Chem. Phys., 20, 6323–6337, https://doi.org/10.5194/acp-20-6323-
- 472 2020, 2020b.
- 473 Liu, Y., Geng, G., Cheng, J., Liu, Y., Xiao, Q., Liu, L., Shi, Q., Tong, D., He, K., and Zhang, Q.: Drivers of Increasing Ozone
- during the Two Phases of Clean Air Actions in China 2013-2020, Environ. Sci. Technol., 57, 8954-8964,
- 475 https://doi.org/10.1021/acs.est.3c00054, 2023.
- 476 Lu, X., Zhang, L., Chen, Y., Zhou, M., Zheng, B., Li, K., Liu, Y., Lin, J., Fu, T.-M., and Zhang, Q.: Exploring 2016–2017
- surface ozone pollution over China: source contributions and meteorological influences, Atmos. Chem. Phys., 19, 8339–
- 478 8361, https://doi.org/10.5194/acp-19-8339-2019, 2019a.
- 479 Lu, X., Zhang, L., and Shen, L.: Meteorology and Climate Influences on Tropospheric Ozone: a Review of Natural Sources,
- 480 Chemistry, and Transport Patterns, Curr. Pollut. Rep., 5, 238–260, https://doi.org/10.1007/s40726-019-00118-3, 2019b.
- 481 Luo, Z., Lu, P., Chen, Z., and Liu, R.: Ozone Concentration Estimation and Meteorological Impact Quantification in the
- 482 Beijing-Tianjin-Hebei Region Based on Machine Learning Models, Earth Space Sci., 11, e2023EA003346,
- 483 https://doi.org/10.1029/2023EA003346, 2024.





- Lyu, X., Li, K., Guo, H., Morawska, L., Zhou, B., Zeren, Y., Jiang, F., Chen, C., Goldstein, A. H., Xu, X., Wang, T., Lu, X.,
- Zhu, T., Querol, X., Chatani, S., Latif, M. T., Schuch, D., Sinha, V., Kumar, P., Mullins, B., Seguel, R., Shao, M., Xue,
- 486 L., Wang, N., Chen, J., Gao, J., Chai, F., Simpson, I., Sinha, B., and Blake, D. R.: A synergistic ozone-climate control to
- address emerging ozone pollution challenges, One Earth, 6, 964–977, https://doi.org/10.1016/j.oneear.2023.07.004, 2023.
- 488 Mao, Y., Shang, Y., Liao, H., Cao, H., Qu, Z., and Henze, D. K.: Sensitivities of ozone to its precursors during heavy ozone
- 489 pollution events in the Yangtze River Delta using the adjoint method, Sci. Total Environ., 925, 171585,
- 490 https://doi.org/10.1016/j.scitotenv.2024.171585, 2024.
- 491 Mousavinezhad, S., Choi, Y., Pouyaei, A., Ghahremanloo, M., and Nelson, D. L.: A comprehensive investigation of surface
- 492 ozone pollution in China, 2015–2019: separating the contributions from meteorology and precursor emissions, Atmos.
- 493 Res., 257, 105599, https://doi.org/10.1016/j.atmosres.2021.105599, 2021.
- 494 Ni, Y., Yang, Y., Wang, H., Li, H., Li, M., Wang, P., Li, K., and Liao, H.: Contrasting changes in ozone during 2019–2021
- between eastern and the other regions of China attributed to anthropogenic emissions and meteorological conditions, Sci.
- 496 Total Environ., 908, 168272, https://doi.org/10.1016/j.scitotenv.2023.168272, 2024.
- 497 Pan, W., Gong, S., Lu, K., Zhang, L., Xie, S., Liu, Y., Ke, H., Zhang, X., and Zhang, Y.: Multi-scale analysis of the impacts
- of meteorology and emissions on PM_{2.5} and O₃ trends at various regions in China from 2013 to 2020 3. Mechanism
- assessment of O₃ trends by a model, Sci. Total Environ., 857, 159592, https://doi.org/10.1016/j.scitotenv.2022.159592,
- 500 2023.
- 501 Qi, G., Che, J., and Wang, Z.: Differential effects of urbanization on air pollution: evidences from six air pollutants in mainland
- 502 China, Ecol. Indic., 146, 109924, https://doi.org/10.1016/j.ecolind.2023.109924, 2023.
- Qian, J., Liao, H., Yang, Y., Li, K., Chen, L., and Zhu, J.: Meteorological influences on daily variation and trend of summertime
- surface ozone over years of 2015–2020: Quantification for cities in the Yangtze River Delta, Sci. Total Environ., 834,
- 505 155107, https://doi.org/10.1016/j.scitotenv.2022.155107, 2022.
- Qiao, W., Li, K., Yang, Z., Chen, L., and Liao, H.: Implications of the extremely hot summer of 2022 on urban ozone control
- 507 in China, Atmospheric and Oceanic Science Letters, 17, 100470, https://doi.org/10.1016/j.aosl.2024.100470, 2024.
- 508 Rao, S. T. and Zurbenko, I. G.: Detecting and tracking changes in ozone air quality, Air Waste, 44, 1089-1092,
- 509 https://doi.org/10.1080/10473289.1994.10467303, 1994.
- 510 Ren, J., Guo, F., and Xie, S.: Diagnosing ozone–NO_x–VOC sensitivity and revealing causes of ozone increases in China based
- on 2013–2021 satellite retrievals, Atmos. Chem. Phys., 22, 15035–15047, https://doi.org/10.5194/acp-22-15035-2022,
- 512 2022.
- 513 Sadeghi, B., Ghahremanloo, M., Mousavinezhad, S., Lops, Y., Pouyaei, A., and Choi, Y.: Contributions of meteorology to
- ozone variations: Application of deep learning and the Kolmogorov-Zurbenko filter, Environ. Pollut., 310, 119863,
- 515 https://doi.org/10.1016/j.envpol.2022.119863, 2022.





- 516 Shang, N., Gui, K., Zhao, H., Yao, W., Zhao, H., Zhang, X., Zhang, X., Li, L., Zheng, Y., Wang, Z., Wang, Y., Che, H., and
- Zhang, X.: Decomposition of meteorological and anthropogenic contributions to near-surface ozone trends in Northeast
- 518 China (2013–2021), Atmos. Pollut. Res., 14, 101841, https://doi.org/10.1016/j.apr.2023.101841, 2023.
- 519 Shen, F., Zhang, L., Jiang, L., Tang, M., Gai, X., Chen, M., and Ge, X.: Temporal variations of six ambient criteria air pollutants
- from 2015 to 2018, their spatial distributions, health risks and relationships with socioeconomic factors during 2018 in
- 521 China, Environ. Int., 137, 105556, https://doi.org/10.1016/j.envint.2020.105556, 2020.
- 522 Shen, L., Liu, J., Zhao, T., Xu, X., Han, H., Wang, H., and Shu, Z.: Atmospheric transport drives regional interactions of ozone
- 523 pollution in China, Sci. Total Environ., 830, 154634, https://doi.org/10.1016/j.scitotenv.2022.154634, 2022.
- 524 Sun, Y., Yin, H., Lu, X., Notholt, J., Palm, M., Liu, C., Tian, Y., and Zheng, B.: The drivers and health risks of unexpected
- surface ozone enhancements over the Sichuan Basin, China, in 2020, Atmos. Chem. Phys., 21, 18589–18608,
- 526 https://doi.org/10.5194/acp-21-18589-2021, 2021.
- 527 Vu, T. V., Shi, Z., Cheng, J., Zhang, Q., He, K., Wang, S., and Harrison, R. M.: Assessing the impact of clean air action on air
- quality trends in Beijing using a machine learning technique, Atmos. Chem. Phys., 19, 11303–11314,
- 529 https://doi.org/10.5194/acp-19-11303-2019, 2019.
- Wang, M., Chen, X., Jiang, Z., He, T.-L., Jones, D., Liu, J., and Shen, Y.: Meteorological and anthropogenic drivers of surface
- ozone change in the North China Plain in 2015–2021, Sci. Total Environ., 906, 167763,
- 532 https://doi.org/10.1016/j.scitotenv.2023.167763, 2024a.
- 533 Wang, P.: China's air pollution policies: progress and challenges, Curr. Opin. Environ. Sci. Health, 19, 100227,
- 534 https://doi.org/10.1016/j.coesh.2020.100227, 2021.
- Wang, T., Xue, L., Brimblecombe, P., Lam, Y. F., Li, L., and Zhang, L.: Ozone pollution in China: a review of concentrations,
- meteorological influences, chemical precursors, and effects, Sci. Total Environ., 575, 1582–1596
- 537 https://doi.org/10.1016/j.scitotenv.2016.10.081, 2017.
- Wang, W., Parrish, D. D., Wang, S., Bao, F., Ni, R., Li, X., Yang, S., Wang, H., Cheng, Y., and Su, H.: Long-term trend of
- ozone pollution in China during 2014–2020: distinct seasonal and spatial characteristics and ozone sensitivity, Atmos.
- 540 Chem. Phys., 22, 8935–8949, https://doi.org/10.5194/acp-22-8935-2022, 2022.
- 541 Wang, X., Jiang, L., Guo, Z., Xie, X., Li, L., Gong, K., and Hu, J.: Influence of meteorological reanalysis field on air quality
- 542 modeling in the Yangtze River Delta, China, Atmos. Environ., 318, 120231,
- 543 https://doi.org/10.1016/j.atmosenv.2023.120231, 2024b.
- Wang, X., Zhu, J., Li, K., Chen, L., Yang, Y., Zhao, Y., Yue, X., Gu, Y., and Liao, H.: Meteorology-driven trends in PM2.5
- concentrations and related health burden over India, Atmos. Res, 2024c.
- 546 Wang, Y., Zhao, Y., Liu, Y., Jiang, Y., Zheng, B., Xing, J., Liu, Y., Wang, S., and Nielsen, C. P.: Sustained emission reductions
- 547 have restrained the ozone pollution over China, Nat. Geosci., 16, 967–974, https://doi.org/10.1038/s41561-023-01284-2,
- 548 2023.





- Wei, J., Li, Z., Li, K., Dickerson, R. R., Pinker, R. T., Wang, J., Liu, X., Sun, L., Xue, W., and Cribb, M.: Full-coverage
- mapping and spatiotemporal variations of ground-level ozone (O₃) pollution from 2013 to 2020 across China, Remote
- 551 Sens. Environ., 270, 112775, https://doi.org/10.1016/j.rse.2021.112775, 2022.
- Weng, X., Forster, G. L., and Nowack, P.: A machine learning approach to quantify meteorological drivers of ozone pollution
- in China from 2015 to 2019, Atmos. Chem. Phys., 22, 8385–8402, https://doi.org/10.5194/acp-22-8385-2022, 2022.
- Weng, X., Li, J., Forster, G. L., and Nowack, P.: Large modeling uncertainty in projecting decadal surface ozone changes over
- city clusters of China, Geophys. Res. Lett., 50, e2023GL103241, https://doi.org/10.1029/2023GL103241, 2023.
- 556 Wise, E. K. and Comrie, A. C.: Extending the Kolmogorov-Zurbenko Filter: Application to Ozone, Particulate Matter, and
- 557 Meteorological Trends, J. Air Waste Manage. Assoc., 55, 1208–1216, https://doi.org/10.1080/10473289.2005.10464718,
- 558 2005.
- 559 Wu, Y., Li D., Zhang L., and Dai H.: Modeling Study on the Impact of Climate Change on Air Pollution. Acta Scientiarum
- 560 Naturalium Universitatis Pekinensis, 59, 854–870. https://doi.org/10.13209/j.0479-8023.2023.010, 2023.
- 561 Yan, D., Jin, Z., Zhou, Y., Li, M., Zhang, Z., Wang, T., Zhuang, B., Li, S., and Xie, M.: Anthropogenically and
- 562 meteorologically modulated summertime ozone trends and their health implications since China's clean air actions,
- 563 Environ. Pollut., 343, 123234, https://doi.org/10.1016/j.envpol.2023.123234, 2024.
- Yao, T., Ye, H., Wang, Y., Zhang, J., Guo, J., and Li, J.: Kolmogorov-Zurbenko filter coupled with machine learning to reveal
- multiple drivers of surface ozone pollution in China from 2015 to 2022, Sci. Total Environ., 949, 175093,
- 566 https://doi.org/10.1016/j.scitotenv.2024.175093, 2024.
- 567 Yin, H., Lu, X., Sun, Y., Li, K., Gao, M., Zheng, B., and Liu, C.: Unprecedented decline in summertime surface ozone over
- 568 eastern China in 2020 comparably attributable to anthropogenic emission reductions and meteorology, Environ. Res. Lett.,
- 569 16, 124069, https://doi.org/10.1088/1748-9326/ac3e22, 2021.
- 570 Zhai, S., Jacob, D. J., Wang, X., Liu, Z., Wen, T., Shah, V., Li, K., Moch, J. M., Bates, K. H., Song, S., Shen, L., Zhang, Y.,
- 571 Luo, G., Yu, F., Sun, Y., Wang, L., Qi, M., Tao, J., Gui, K., Xu, H., Zhang, Q., Zhao, T., Wang, Y., Lee, H. C., Choi, H.,
- 572 and Liao, H.: Control of particulate nitrate air pollution in China, Nat. Geosci., 14, 389-395,
- 573 https://doi.org/10.1038/s41561-021-00726-z, 2021.
- 574 Zhang, L., Wang, L., Liu, B., Tang, G., Liu, B., Li, X., Sun, Y., Li, M., Chen, X., Wang, Y., and Hu, B.: Contrasting effects
- of clean air actions on surface ozone concentrations in different regions over Beijing from May to September 2013–2020,
- 576 Sci. Total Environ., 903, 166182, https://doi.org/10.1016/j.scitotenv.2023.166182, 2023.
- 577 Zhang, Y., Lei, R., Cui, S., Wang, H., Chen, M., and Ge, X.: Spatiotemporal trends and impact factors of PM_{2.5} and O₃ pollution
- in major cities in China during 2015–2020, Chin. Sci. Bull., 67, 2029–2042, https://doi.org/10.1360/TB-2021-0767,
- 579 2022a.
- 580 Zhang, Z., Xu, B., Xu, W., Wang, F., Gao, J., Li, Y., Li, M., Feng, Y., and Shi, G.: Machine learning combined with the PMF
- model reveal the synergistic effects of sources and meteorological factors on PM_{2.5} pollution, Environ. Res., 212, 113322,
- 582 https://doi.org/10.1016/j.envres.2022.113322, 2022b.





- Zhao, S., Yin, D., Yu, Y., Kang, S., Qin, D., and Dong, L.: PM_{2.5} and O₃ pollution during 2015–2019 over 367 Chinese cities:
- 584 spatiotemporal variations, meteorological and topographical impacts, Environ. Pollut., 264, 114694,
- 585 https://doi.org/10.1016/j.envpol.2020.114694, 2020.
- Zuo, C., Chen, J., Zhang, Y., Jiang, Y., Liu, M., Liu, H., Zhao, W., and Yan, X.: Evaluation of four meteorological reanalysis
- 587 datasets for satellite-based PM_{2.5} retrieval over China, Atmos. Environ., 305, 119795,
- 588 https://doi.org/10.1016/j.atmosenv.2023.119795, 2023.